

# Measurement and analysis of dynamic instabilities in fluid-heated two-phase flow

D. M. FRANCE,\* R. D. CARLSON and R. P. ROY†

Argonne National Laboratory, 9700 South Cass Avenue, Argonne, IL 60439, U.S.A.

(Received 30 December 1985 and in final form 21 March 1986)

**Abstract**—Dynamic, density wave, stability experiments were performed using high-pressure boiling water and liquid heating. Liquid sodium at temperatures up to 500°C provided heat to boil water at pressures of 7–16 MPa and mass fluxes of 170–800 kg m<sup>-2</sup> s<sup>-1</sup>. Water flowed inside a vertical tube, with a heated length of 13 m, and exited superheated in all tests. Special attention was given to the test procedure used to approach instability, and stability thresholds were determined. Experimental results were compared with predictions from the DYNAM computer code and two recent correlation equations. One of the equations was successfully modified to predict the experimental results well.

## INTRODUCTION

MANY types of flow instabilities have been observed and defined in two-phase flows, as summarized in refs. [1, 2]. Of particular interest to this investigation is the dynamic instability most common to parallel channel two-phase flows. This density wave feedback instability is characterized by large amplitude, low frequency flow oscillations in the boiling fluid. These oscillations have been observed to culminate in either a limit cycle condition or a flow excursion. Both consequences are undesirable in physical systems, and avoidance is dependent upon knowledge of conditions at the threshold of the instability.

Many techniques have been developed for prediction of dynamic stability thresholds including stability maps, empirical and phenomenological correlations, and large computer analyses in both the frequency and time domains. The data, upon which these techniques were based or against which they were verified, are most prevalent from heat flux controlled experiments. The specific system of interest to this investigation is temperature controlled by means of fluid heating. In this case, heating may be controlled by either heating fluid temperature or flowrate. Data from such temperature controlled systems are considerably less numerous than from heat flux controlled experiments. The objectives of this investigation were to obtain dynamic stability threshold data in a temperature controlled, high pressure, boiling water system and to compare results to predictions from techniques that were developed for application to such systems and had employed temperature controlled system data in their development.

Experiments were performed in the Steam Generator Test Facility (SGTF) at Argonne National Laboratory (ANL) where water was boiled at pressures of 7–16 MPa and flows of 170–800 kg m<sup>-2</sup> s<sup>-1</sup> as it flowed upwards inside a vertical tube. Heat was supplied from countercurrent-flowing liquid sodium at temperatures up to 500°C. Parameters at the threshold of density wave instability were determined in each test using test section inlet and outlet throttling to approach instability. The experimental results were compared with three methods of threshold prediction for density wave instabilities.

- (1) The DYNAM computer code [3] using two methods of comparison.
- (2) The semi-empirical correlation equation of Ünal [4] and a modified version of this equation.
- (3) A recent technique [5] that was reported to be more accurate than the Ünal equation.

Both correlation equations and detailed predictive computer codes are used for the assessment of stability thresholds depending upon the application. Correlation equations are especially useful in determining whether a system is very stable, very unstable, or marginally stable wherein a code such as DYNAM might be applied for further refinement. The data comparisons with correlations and computer code provide accuracy verification for the current application of liquid-heated, high-pressure boiling water. In the case of the Ünal equation, the data were utilized in the development of a modified version of it.

## EXPERIMENTAL APPARATUS

The SGTF employs sodium to boil water in the test section. The SGTF will accommodate test sections with vertical lengths more than 21 m, and the sodium and water circuits are shown in Fig. 1. The electric power supply and electromagnetic sodium pump have

\* Presently at the University of Illinois at Chicago, Chicago, IL 60680, U.S.A.

† Presently at Arizona State University, Tempe, AZ 85287, U.S.A.

## NOMENCLATURE

$C$ and $C_c$	correlation parameters defined in equations (9) and (10)	$L$	heated length [m]
$d$	water tube inside diameter [m]	$P$	steam pressure [MPa]
$G$	water mass flux [ $\text{kg m}^{-2} \text{s}^{-1}$ ]	$P_r$	reduced pressure
$\Delta H$	dimensionless inlet subcooling enthalpy (1 – enthalpy at inlet/enthalpy of saturated liquid)	$Re_v$	Reynolds number of saturated vapor
$K_i$	inlet throttling coefficient, pressure drop/ ( $\frac{1}{2}$ density $\times$ velocity squared)	$T_{\text{Na,inlet}}$	sodium inlet temperature to the test section [ $^{\circ}\text{C}$ ]
$K_e$	exit throttling coefficient, pressure drop/ ( $\frac{1}{2}$ density $\times$ velocity squared)	$T_{\text{sat}}$	water saturation temperature [ $^{\circ}\text{C}$ ]
		$W_n/W_w$	ratio of mass flowrate of sodium to mass flowrate of water ( $\text{kg s}^{-1}$ )/( $\text{kg s}^{-1}$ )
		$X$	exit water quality at the inception of instability.

maximum capacities of 1 MW and  $0.0044 \text{ m}^3 \text{ s}^{-1}$  at  $650^{\circ}\text{C}$ . The water circuit is shown in Fig. 1 operating in the recirculation mode with saturated water/steam flowing vertically upward from the test section to a separation tank (steam drum). Steam from the top of

the drum is condensed in the condenser; the liquid from the bottom of the drum is subcooled in another heat exchanger (cooler).

The water temperature at the test section inlet is controlled by the heat rejection of the cooler and

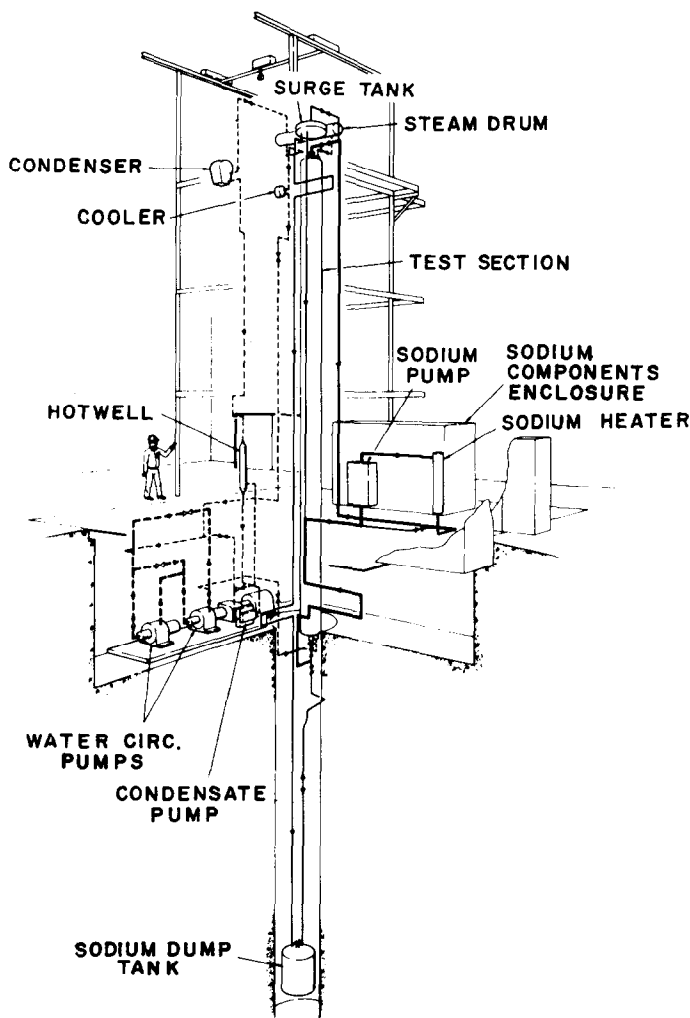


FIG. 1. Steam Generator Test Facility.

condenser. This dual heat exchanger (condenser and cooler) heat rejection system precludes the need for a high-pressure water preheater. The condensate and water from the cooler are recombined before entering the canned-rotor, high-pressure, centrifugal-pump circuit from which the flow enters the test section through a throttling valve. The water circuit has maximum pressure and flow ratings of 16.5 MPa and  $0.0082 \text{ m}^3 \text{ s}^{-1}$ .

A somewhat unique aspect of the SGTF is the condenser/cooler arrangement with both components at full system pressure. To maintain fine system control with fast feedback, a high-temperature synthetic oil is used as the heat rejection fluid in the condenser and cooler; the oil in turn rejects heat to a water cooling tower. The oil system, not shown in Fig. 1, uses pneumatically controlled valves to change load quickly by changing oil flow rather than temperature.

The stability experiments all were performed with superheated steam exiting the test section. For these tests, a desuperheating heat exchanger with very low pressure drop was added just below the steam drum. The system continued to operate in the recirculation

mode. This configuration subjected only a short segment of piping to high superheat temperature; only this segment was upgraded for the tests.

Water valves positioned close to the test section inlet and outlet were used as variable orifices. The inlet and/or outlet throttlings were changed during a test by adjusting these two valves; the test section flowrate was independent of the settings. (The test section water flowrate could be maintained at any value, using the pump circuit valves, independent of the inlet and outlet throttlings.) This arrangement gave the system considerable versatility in the approach to instability.

Investigation of parallel channel flow instability requires the imposition of constant pressures, independent of flow, at the test section inlet upstream of the throttle valve and at the test section outlet downstream of the throttle valve. These pressure boundary conditions were realized in the SGTF by a combination pressure control and parallel piping.

The test section, shown in Fig. 2, consists of a  $2\frac{1}{4}$  Cr-1 Mo steel tube with inside diameter of 10.1 mm and wall thickness of 2.90 mm, in which water flows

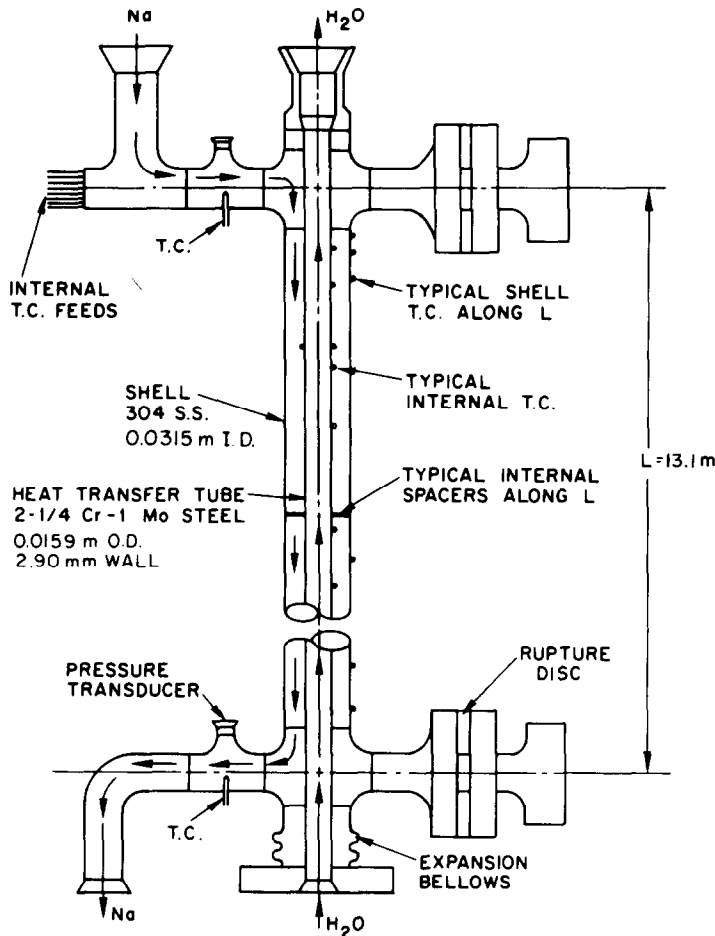


FIG. 2. SGTF test section.

vertically upward. Sodium flows countercurrent in the annulus between the water tube and the Type 304 stainless-steel sodium shell (31.5 mm ID). The tubes are held in concentricity by support spacers designed for minimum heat transfer between tubes and minimum flow perturbation. The heat transfer length between centerlines of the sodium nozzles is 13.1 m.

One hundred and two shell thermocouples are spot-welded axially along the outside of the sodium tube (shell), with a minimum spacing of 0.076 m. These thermocouple measurements were used with measured pressures and flows to determine local parameters at the thresholds of instabilities. The SGTF and test section are described further in ref. [6].

### EXPERIMENTAL PROCEDURE

The technique most commonly used for approaching dynamic instability in an experimental system is to start from a steady-state condition and to lower the water flowrate until instability is reached. This approach to instability causes rather large hydrodynamic and thermal perturbations in the test section. Lowering the water flowrate in a once-through system causes the critical heat flux to move upstream, which causes large changes in tube wall temperature in its vicinity. In a sodium-heated test section, the sodium temperature and heat flux distributions also will be affected. As a result of these changes, the system can be forced into instability prematurely. An alternate approach to instability was used in this investigation which minimized parametric perturbation and premature instabilities.

All tests in this study were initiated from a predetermined steady-state condition. The five parameters that specify a test are water flowrate, pressure and inlet temperature, and sodium flowrate and inlet temperature. All these parameters were held approximately constant throughout each test. In most tests, there was no exit throttling and substantial inlet throttling at the initial steady-state operating condition. This arrangement yielded very steady water flow. Subsequently, the throttlings were altered in the direction of instability in small increments while maintaining all other parameters approximately constant, including the water flowrate. Using this procedure, there was essentially no perturbation to fluid temperature, heat flux, etc. in the test section. The throttlings continued to be changed in this way (decreasing inlet throttling and/or increasing exit throttling) until the threshold of instability was reached, and data were recorded by a computerized data acquisition system. Subsequently, the throttlings were changed again, producing the large water flowrate fluctuations of dynamic instability that were important to verify that the threshold had been reached.

There is another advantage to the test procedure employed in this study. It allowed stability thresholds to be determined at specified water flowrates. Essentially, throttlings were sought that produced the

threshold of dynamic instability of a predetermined range of water flowrate and system operating conditions. The approach to instability that decreases water flowrate cannot predetermine the test section condition when instability is reached. Approaching instability in the SGTF using the water flowrate reduction technique verified the experience of other investigators that it was necessary to produce a very slow, quasi-steady transient which, in some parameter ranges, became difficult to maintain as a consequence of facility control limitation. For these reasons, the throttling approach to instability was considered to be the preferable technique, and it was used in all tests of this investigation.

Data at and beyond the threshold of instability also were recorded on an FM magnetic tape recorder. These analog recordings were used to reproduce the time variations of various test section parameters. Some of them were digitized and subjected to spectral analysis.

### RESULTS

Results from Test 960 were chosen as an example of the threshold of dynamic instability. The water mass flux during the test is shown in Fig. 3. As discussed previously, the throttlings were changed in small increments during the test while initial flow, temperature, and pressure conditions were maintained. The water mass flux at the threshold of instability is shown in Fig. 3 for the time increment of 0–125 s. At 125 s, the throttlings were changed again, as indicated in Fig. 3, resulting in large-amplitude oscillations. Before this final throttling change, the water mass flux was relatively constant, with small-amplitude fluctuations that appeared and disappeared with time. After the throttling change, the fluctuations became pronounced, with a clear dominant frequency. The amplitude increased with each cycle until it reached more than 100% of the initial mean mass flux. (In some experiments, a limit cycle was reached at moderate to large amplitudes.) The flow oscillations shown in Fig. 3 led to flow reversal, and the test was terminated.

A second example of typical stability test results is given in Figs. 4 and 5. The stability threshold was somewhat different from that in Fig. 3. A throttling change was made at the point indicated as the threshold of instability in Fig. 4. Subsequently, small-amplitude fluctuations appeared in the water flowrate. The fluctuations are seen in Fig. 4 to have a clear dominant frequency, but the amplitude did not grow to very large values, as in the test results in Fig. 3. However, the next throttling change produced the increased amplitude shown in Fig. 5 that led to a limit cycle with fluctuation amplitude of 100% of the mean water flow. The throttling increment between Figs. 4 and 5 was on the order of 5 kPa.

Spectral analysis was performed on a segment of flow fluctuations of moderate amplitude similar to

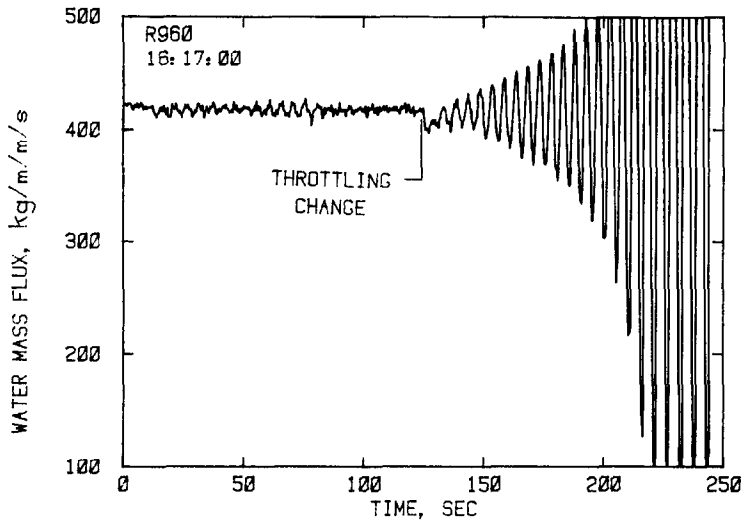


FIG. 3. Stability threshold and beyond.

the early stages shown in Fig. 5. The power spectral density is shown in Fig. 6, where it is clear that a frequency of 0.23 Hz dominates the spectrum. Higher-frequency components were present in much smaller amplitudes.

These results for water flowrate fluctuations at and beyond the threshold of dynamic instability are similar to instabilities found by other investigators in both liquid-heated and heat-flux-imposed systems that were attributed to density wave feedback. Examples of similar measurements in liquid-heated systems are given in refs. [7-9]. The frequency of the instabilities were predicted reasonably well by the DYNAM com-

puter code as noted in ref. [10]. It is for these reasons that the instabilities encountered in this investigation are considered to be of the density wave type.

Data were recorded at the threshold point for each test performed. The temperature, flow and pressure measurements were analyzed to produce a full set of parametric conditions, including axial heat flux, at the instability thresholds.

**COMPARISON WITH DYNAM**

Representative tests covering the water flow and pressure range of the experiments were analyzed by

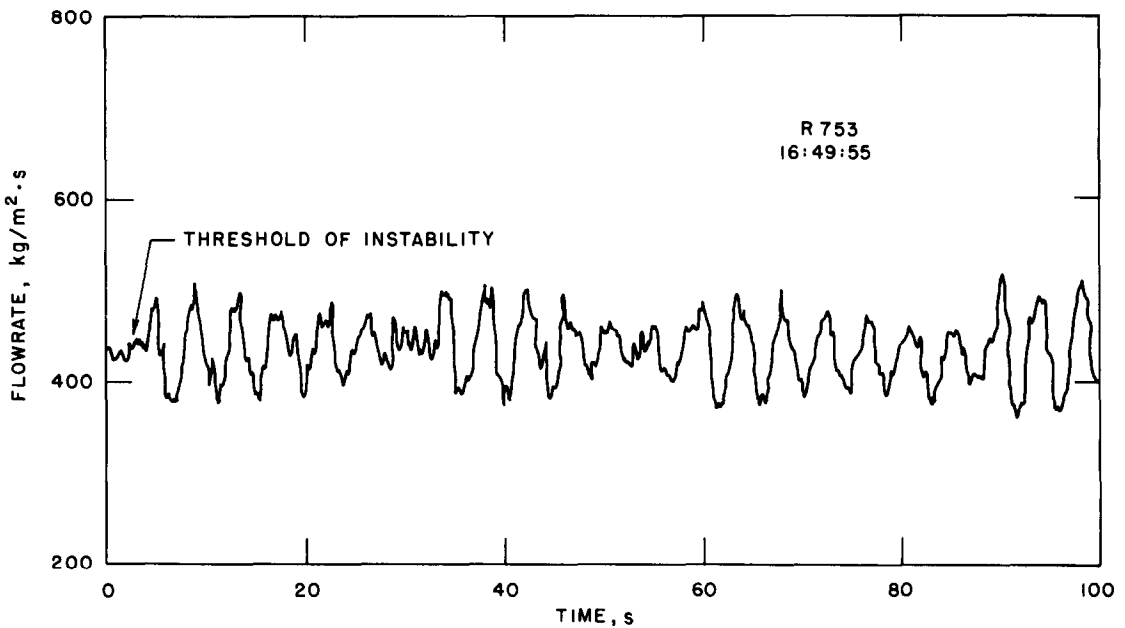


FIG. 4. Dynamic stability threshold.

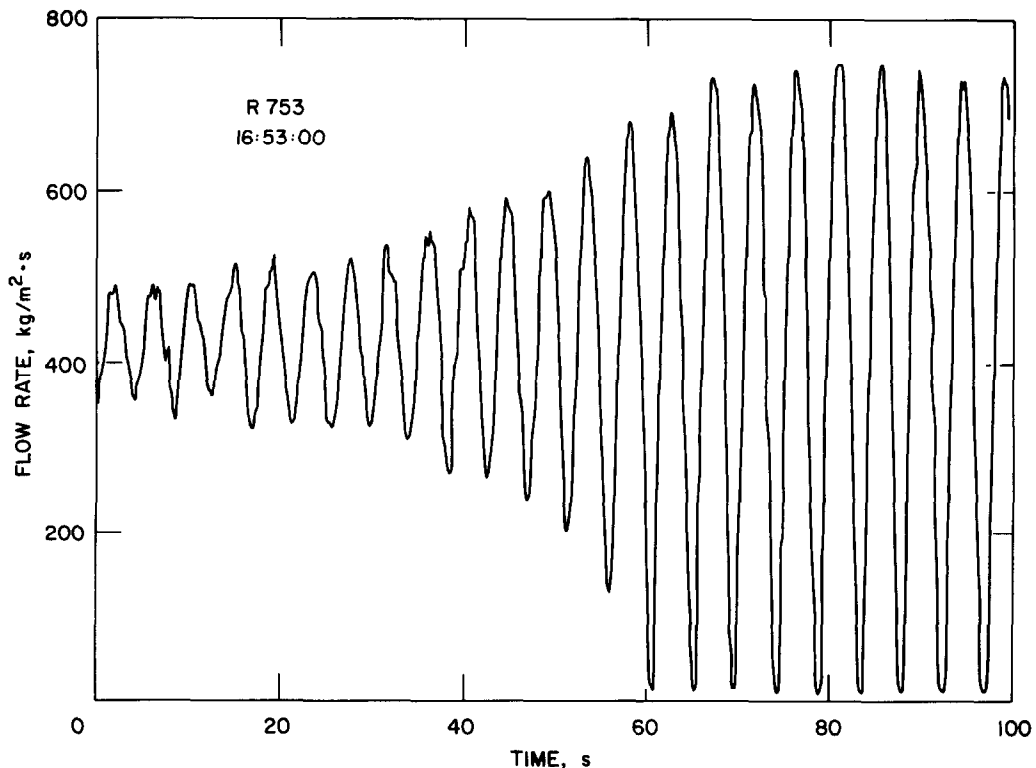


FIG. 5. Large-amplitude dynamic instability flow fluctuation.

the DYNAM computer code. The DYNAM code was chosen from among several existing codes for density wave stability analysis because it is a well-established code that has been used for high-pressure water flow systems for many years. The code predicts the threshold of density wave instability using a frequency domain analysis. Two-phase flow and superheated vapor regions are included as well as the effects of inlet and outlet throttling. (The instability frequency is also predicted by DYNAM as discussed previously.)

Comparisons of measured and predicted stability thresholds were made in two ways. In the first comparison, all system conditions at the experimental stability threshold were input to DYNAM except for the pressure drop across the test section inlet throttle valve. DYNAM predicted the inlet pressure drop (throttling) at the threshold of instability that could be compared with the measured value. The use of DYNAM in this way was similar to the experimental procedure.

The predicted inlet throttlings (DP-IN in Fig. 7) were compared with the experimental values. The comparison is good, with points well centered about the perfect agreement line (the 45° line in Fig. 7). Points lying to the right of this line are conservative predictions; nonconservative are to the left. Although the points in Fig. 7 are distributed almost equally between conservative and nonconservative predictions, DYNAM predictions were systematic with respect to water pressure. Predicted inlet throttling

was found to be consistently conservative at the high pressure of 16 MPa and nonconservative at the low pressure of 7 MPa.

The second method of comparing DYNAM predictions with experimental data was similar to the method discussed above except that the measured inlet throttlings at the stability thresholds were input into DYNAM, and the outlet throttlings were predicted. The results of the comparison are shown in Fig. 8, where DP-OUT is the exit throttling. The axes in Fig. 8 were changed, compared with Fig. 7, so that conservative predictions still fall to the right of the 45° line in Fig. 8. Although the points in Fig. 8 are distributed relatively evenly with respect to conservative and nonconservative predictions, the scatter in Fig. 8 is significantly larger than in Fig. 7.

The same systematic deviations between DYNAM predictions and measurements were found for the exit throttling as for the inlet throttling case. The predictions were conservative at high pressure and nonconservative at low pressure. No systematic error was found with respect to water mass flux in either inlet or exit throttling predictions.

## COMPARISON WITH CORRELATIONS

### *Ünal correlation*

Ünal's correlation equation [4] for predicting the threshold of density wave instabilities in once-through, sodium-heated, high-pressure boiling water

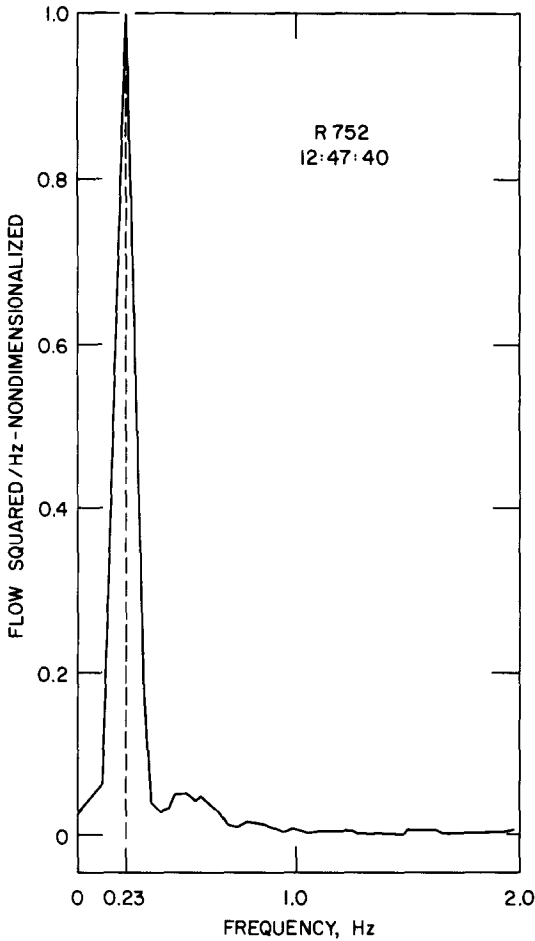


FIG. 6. Power spectral density of water flow fluctuation.

was compared with the SGTF data. It was determined that the equation had the potential for correlating the data except for the parameter range of the highest pressure (16 MPa) and the lowest water mass flux ( $170 \text{ kg m}^{-2} \text{ s}^{-1}$ ). Thus, data in the range shown in Fig. 9 were used for comparison with Ünal's equation.

Ünal's equation predicts the water quality at the instability threshold, given the test section and inlet throttling conditions. The equation has the form

$$X = A_1 A_2 A_3 A_4 A_5 A_6 \quad (1)$$

where  $X$  is the thermodynamic equilibrium water quality at the test section exit; it may be greater than unity. The  $A$  terms of equation (1) represent the effects of pressure, flowrate, inlet water subcooling, vapor Reynold's number, inlet throttling and geometry. Equation (1) is compared with data from the SGTF test series in Fig. 10. The majority of the measured data are overpredicted by equation (1). This result is nonconservative, and the high-pressure, low-flow results omitted from the comparison were predicted very conservatively. In general, the comparison of Fig. 10 was encouraging, and a modification of Ünal's equation was developed to better predict the SGTF data while retaining the general form and parameter groups in the equation. Also, an additional term was added to account for exit throttling. The following equation resulted:

$$X = B_1 B_2 B_3 B_4 B_5 B_6 B_7 \quad (2)$$

The pressure dependence of equation (1) produced a systematic deviation between predictions and SGTF data. The pressure dependence term,  $A_1$ , was modified to  $B_1$ , where

$$B_1 = 0.131 - 0.125 \ln [(1 - P_r) P_r^{0.3}] \quad (3)$$

A similar systematic dependence was found with respect to flowrate ratio. The flow ratio term,  $A_2$ , was modified to  $B_2$ , where

$$B_2 = 1 - 0.008 W_n / W_w \quad (4)$$

The subcooling and Reynold's number terms were unchanged:

$$B_3 = A_3 = 1 + 0.13 \Delta H \quad (5)$$

and

$$B_4 = A_4 = Re_v^{0.125} \quad (6)$$

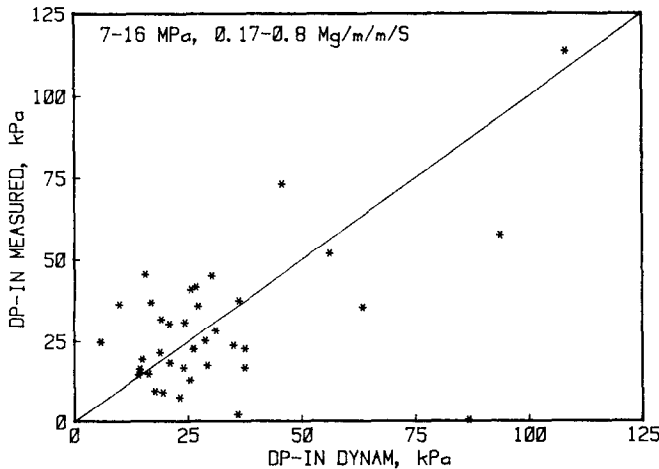


FIG. 7. DYNAM inlet throttling predictions.

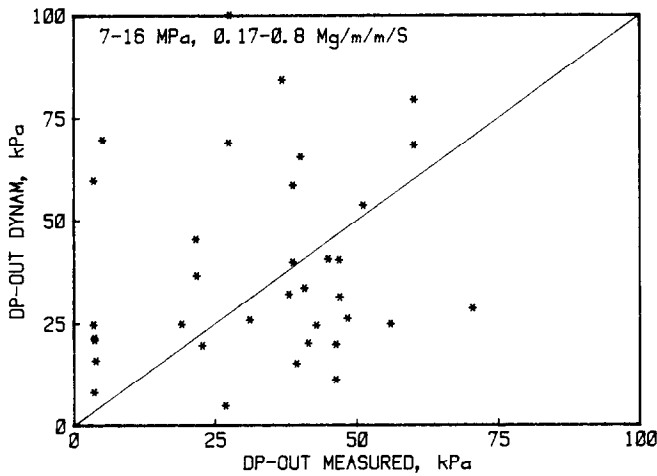


FIG. 8. DYNAM outlet throttling predictions.

Systematic deviations were encountered between predictions of equation (1) and SGTF data with respect to inlet throttling. The deviations had opposite signs at low and high inlet throttlings, so the  $A_5$  term was rotated around moderate throttlings to give  $B_5$

$$B_5 = \left[ 1 + \frac{200K_1}{(L/d)^{0.37}} \right]^{0.0323} \quad (7)$$

The term  $A_6 = B_6 = 1.0$  for straight tubes, and the exit throttling term  $B_7$  was added

$$B_7 = 1 / \left[ 1 + \frac{K_e}{(L/d)^{0.37}} \right]^n \quad (8)$$

where  $n = 0.0001706G - 0.0283$  ( $G$  is in  $\text{kg m}^{-2} \text{s}^{-1}$ ).

The predictions of the modified Ünal equation, equation (2), were compared with the tests in the range shown in Fig. 9. The results are shown in Fig. 11; agreement is very good. All the modifications to equation (1) contributed to this improved prediction. Although equation (1) does not account for exit throttling, and some of the ANL data had exit throttling at the stability threshold, the addition of the  $B_7$  term alone was not capable of producing the results shown in Fig. 11.

*Essen correlation*

Several dynamic stability correlations were compared with test data from sodium-heated experiments

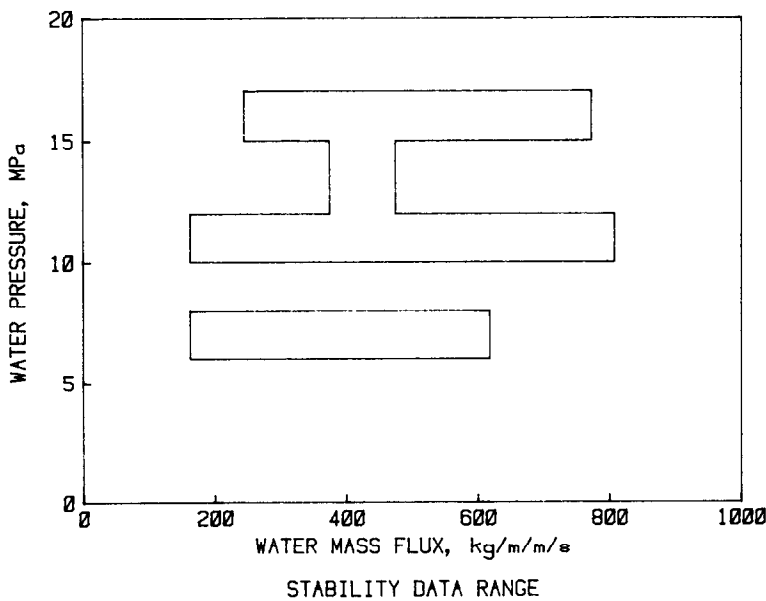


FIG. 9. Data range for comparison with Ünal correlation.



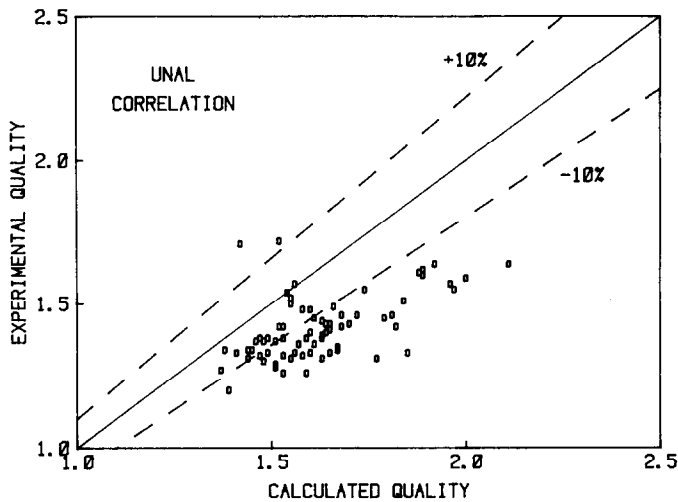


FIG. 10. Data comparison with Ünal correlation.

[5]. Ünal's equation [4] was included. The conclusion was that none of the equations predicted the data well. A new equation was offered that correlated the data better, but the Essen correlation [5] does not include inlet or exit throttling.

The Essen correlation is composed of two equations:

$$C = \frac{W_n}{W_w} (T_{N_{inlet}} - T_{sat}) \quad (9)$$

and

$$C_c = 1074 + 23.4P. \quad (10)$$

Essen compared the predictions of equations (9) and (10) to measurements by computing the 'scatter' defined as

$$\text{scatter} = \frac{C - C_c}{C_c} \times 100\%. \quad (11)$$

The scatter was calculated [5] for each experiment and plotted against the number of experiments, i.e. the data frequency. The same procedure was followed in comparing equation (11) with the SGTF experiments. The results are shown in Fig. 12, in which the plotting limits on scatter are the same as used by Essen. Good agreement would be represented in Fig. 12 by a high

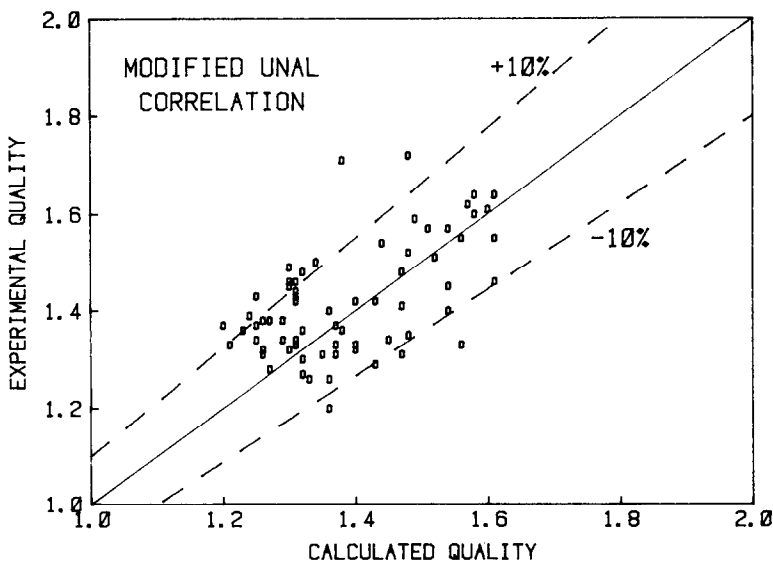


FIG. 11. Data comparison with modified Ünal correlation.

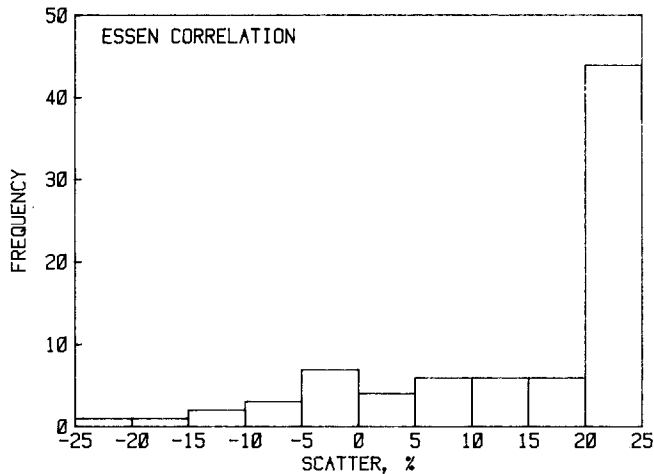


FIG. 12. Data comparison with Essen correlation.

frequency at zero scatter. However, most of the data fell above 20% scatter, indicating poor correlation.

### CONCLUSIONS

The dynamic stability experiments conducted in the SGTF covered a large range of water flowrate and pressure with superheated steam at the test section exit. Instabilities of the density wave type were encountered in all tests, using an approach to instability that minimized system perturbations that can cause premature instabilities.

The comparison of measured stability thresholds with the predictions of the DYNAM computer code produced several important results. In general, the DYNAM predictions compared well with the measurements on the basis of inlet throttling. The comparison with respect to exit throttling was not nearly as good. In both cases, the DYNAM predictions were conservative at high pressure and non-conservative at low pressure.

Ünal's correlation equation [4] was modified successfully to predict the SGTF data very well except for the highest pressure and lowest flow parameter range. The modified Ünal equation [equation (2)] is recommended for use in the parameter range shown in Fig. 9.

The recent correlation of Essen [5] was shown to be in poor agreement with the SGTF data. The absence of both inlet and exit throttling terms in this correlation makes its range of applicability very limited.

### REFERENCES

1. J. S. Bouré, A. E. Bergles and L. S. Tong, Review of two-phase flow instability, *Nucl. Engng Des.* **25**, 165-192 (1973).
2. A. E. Bergles, Instabilities in two-phase flow systems. In *Two-phase Flow and Heat Transfer in Power and Process Industry*. Hemisphere, Washington, DC (1981).
3. L. E. Efferding, DYNAM, a digital computer program for study of the dynamic stability of once-through boiling flow with steam superheat, GAMD-8656, Gulf General Atomic Corp. (1968).
4. H. C. Ünal, Density-wave oscillations in sodium heated once-through steam generator tubes, *J. Heat Transfer* **103**, 485-491 (1981).
5. D. V. Essen and I. T. Kuijper, Calculations on hydrodynamic stability correlations presented in literature, ASME Paper No. 83-WA/NE-8 (1983).
6. D. M. France, R. D. Carlson, T. Chiang and R. Priemer, Characteristics of transition boiling in sodium-heated steam generator tubes, *J. Heat Transfer* **101**, 270-275 (1979).
7. R. P. Waszink and L. E. Efferding, Hydrodynamic stability and thermal performance tests of a 1 MW sodium-heated once-through steam generator model, ASME Paper No. 73-Pwr-16 (1974).
8. H. C. Ünal, M. L. G. von Gasselt and P. W. P. H. Ludwig, Dynamic instabilities in tubes of a large capacity, straight-tube, once-through, sodium-heated steam generator, *Int. J. Heat Mass Transfer* **20**, 1389-1399 (1977).
9. M. Okamachi, T. Tsuchiya and A. Azume, The evaluation methods of the dynamic model for the sodium heated steam generator, *Proc. IAEA* (1979).
10. R. P. Roy, R. C. Dykhuizen, D. M. France and S. P. Kalra, Model predictions of dynamic instability threshold for boiling flow systems, *Trans. Am. nucl. Soc.* **49**, 473-474 (1985).

## MESURE ET ANALYSE DES INSTABILITES DANS UN ECOULEMENT DIPHASIQUE CHAUFFE PAR UN FLUIDE

**Résumé**—Des expériences de stabilité dynamique d'onde de densité sont conduites pour le chauffage d'eau bouillante par un liquide. Le sodium liquide, jusqu'à des températures de 500°C, fournit la chaleur à de l'eau en ébullition à des pressions de 7–16 MPa et à des débits surfaciques de 170–800 kg m<sup>-2</sup> s<sup>-1</sup>. L'eau s'écoule dans un tube vertical, avec une longueur chauffée de 13 m et elle sort surchauffée dans tous les essais. Une attention spéciale est portée à la procédure choisie pour approcher l'instabilité. Les résultats expérimentaux sont comparés avec les prévisions d'une code de calcul DYNAM et avec deux formules récentes. Une de ces formules est modifiée pour représenter correctement les résultats expérimentaux.

## DYNAMISCHE INSTABILITÄTEN IN EINER FLÜSSIGKEITSBEHEIZTEN ZWEIPHASENSTRÖMUNG

**Zusammenfassung**—Untersucht wurden dynamische Instabilitäten, besonders Dichtewellen, an unter hohem Druck siedendem Wasser bei Beheizung mit einer Flüssigkeit. Flüssiges Natrium bei Temperaturen bis zu 500°C diente als Beheizung, um Wasser bei Drücken von 7–16 MPa und Massenstromdichten von 170–800 kg m<sup>-2</sup> s<sup>-1</sup> zu verdampfen. Das Wasser strömte innerhalb eines vertikalen Rohres mit einer beheizten Länge von 13 m, und man erhielt bei allen Versuchen überhitzten Dampf. Besondere Aufmerksamkeit galt den Versuchsabläufen zum Erreichen der Instabilität; die Stabilitätsgrenzen wurden bestimmt. Die experimentellen Ergebnisse wurden sowohl mit Berechnungen nach dem DYNAM-Computer-Program als auch mit zwei neueren Korrelationsgleichungen verglichen. Eine der beiden Gleichungen wurde (erfolgreich) abgeändert, so daß die experimentellen Ergebnisse gut vorausgesagt werden können.

## ИЗМЕРЕНИЕ И АНАЛИЗ ДИНАМИЧЕСКИХ НЕУСТОЙЧИВОСТЕЙ В НАГРЕВАЕМОМ ДВУХФАЗНОМ ПОТОКЕ ЖИДКОСТИ

**Аннотация**—Проведены эксперименты по динамике, волнам сжатия и устойчивости при кипении воды и нагреве жидкости при высоком давлении. Жидкий натрий при температурах до 500°C дает тепло для кипения воды при давлениях 7–16 МПа и массовых потоках 170–800 кг м<sup>-2</sup> с<sup>-1</sup>. Вода текла внутри вертикальной трубы с длиной нагрева 13 м и выходила перегретой во всех опытах. Особое внимание уделено экспериментальной методике, применяемой для изучения начала неустойчивости; были определены пороги устойчивости. Результаты экспериментов сравнивались с расчетами на ЭВМ по программе DYNAM и двумя обобщающими уравнениями. Одно из уравнений модифицировано для достижения хорошего соответствия с экспериментальными результатами.